K. Witrisal, "OFDM Air-Interface Design for Multimedia Communications", Ch. 4, Ph.D. Thesis, Delft University of Technology, The Netherlands, April 2002

Chapter 4 – OFDM Introduction and System Modeling

4.1 Introduction

The aim of this chapter is to provide some theoretical background on the OFDM transmission technique, which is the general topic of the rest of this thesis. A brief introduction to OFDM is given in Section 4.2. We review the block diagram of a "classic" OFDM system, which employs a guard interval to mitigate the impairments of the multipath radio channel. We also discuss several design considerations related to hardware properties and derive the mathematical model for an idealized system, leading to the conclusion that data symbols can be transmitted independently of each other (i.e., without inter-symbol-interference (ISI) and inter-carrier-interference (ICI).) Moreover, the effects of synchronization imperfections are analyzed, like carrier frequency and phase offsets, and timing errors.

Section 4.3 introduces a method of calculating uncoded BERs for this idealized OFDM system model. This method is largely based on work presented in [1]. Differential and coherent detection schemes can be evaluated for Rayleigh and Ricean fading channels. The results obtained are used in later chapters as a benchmark, in order to evaluate the loss of implemented algorithms for the OFDM modems. We also show that, for the system proposal under investigation, differential detection in time-direction is much preferable to differential detection in frequency direction. Imperfect synchronization and channel estimation may be assessed by extending the system model used and by incorporating the SNR degradations due to ICI and ISI. Basic aspects are discussed in this chapter. Issues for a further refinement of the methods are addressed.

The rest of this chapter is organized as follows. The introduction to OFDM and the

derivation of the simplified system models are presented in Section 4.2. In Section 4.3, the performance evaluation of the uncoded OFDM system is outlined, followed by conclusions and recommendations in Section 4.4.

4.2 OFDM Introduction and System Model

Orthogonal frequency division multiplexing (OFDM) is a parallel transmission scheme, where a high-rate serial data stream is split up into a set of low-rate sub-streams, each of which is modulated on a separate sub-carrier (SC) (frequency division multiplexing). Thereby, the bandwidth of the sub-carriers becomes small compared with the coherence bandwidth of the channel, i.e., the individual sub-carriers experience flat fading, which allows for simple equalization. This implies that the symbol period of the sub-streams is made long compared to the delay spread of the time-dispersive radio channel.

Selecting a special set of (orthogonal) carrier frequencies, high spectral efficiency is obtained, because the spectra of the sub-carriers overlap, while mutual influence among the sub-carriers can be avoided (see Figure 1-3 in Chapter 1). The derivation of the system model shows that, by introducing a cyclic prefix (the so-called guard interval (GI)), the orthogonality can be maintained over a dispersive channel (see Section 4.2.3).

This section starts with a brief introduction to the OFDM transmission technique, based on the description of the system's block diagram. We then discuss some hardware-related design considerations (Section 4.2.2) that become relevant if an OFDM system is implemented in hardware. For instance the DC-subcarrier and sub-carriers near the Nyquist-frequency must be avoided. Next, we derive the system model for a perfectly synchronized system (Section 4.2.3), and we investigate the impact of the most relevant synchronization errors (Section 4.2.4).

For a more elaborate introduction to OFDM, the reader may refer to the respective chapters of [2], [3], and to [4]–[6]. An excellent overview over the effects of many non-ideal transmission conditions is given in [7], wherein numerous further references are found.

4.2.1 OFDM Introduction and Block Diagram

Figure 4-1 shows the block diagram of a simplex point-to-point transmission system using OFDM and forward error correction coding. The three main principles incorporated are:

- The *inverse discrete Fourier transform* (IDFT) and the *discrete Fourier transform* (DFT) are used for, respectively, modulating and demodulating the data constellations on the orthogonal sub-carriers [8]. These signal processing algorithms replace the banks of I/Q-modulators and -demodulators that would otherwise be required.

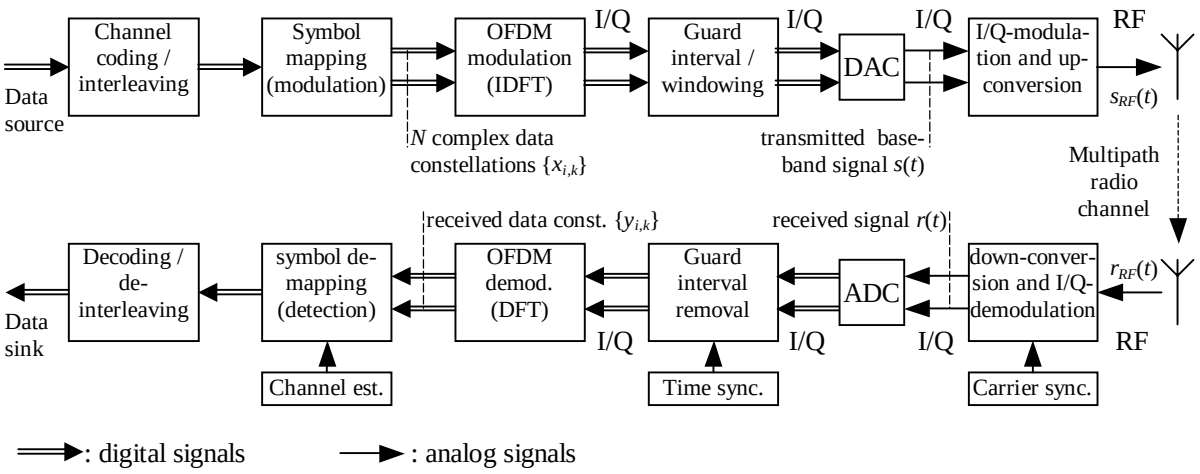

Figure 4-1: Simplex, point-to-point transmission using OFDM.

The analysis of Section 4.2.3 will show this equivalence.

Note that at the input of the IDFT, N data constellation points $\{x_{i,k}\}$ are present, where N is the number of DFT points. (i is an index on the sub-carrier; k is an index on the OFDM symbol). These constellations can be taken according to any phase-shift-keying (PSK) or quadrature-amplitude-modulation (QAM) signaling set (*symbol mapping*). The N output samples of the IDFT – being in time-domain – form the base-band signal carrying the data symbols on a set of N orthogonal sub-carriers. In a real system, however, not all of these N possible sub-carriers can be used for data, as elaborated in Section 4.2.2.3.

Usually, N is taken as an integer power of two, enabling the application of the highly efficient (inverse) fast Fourier transform (IFFT; FFT) algorithms for modulation and demodulation.

- The second key principle is the introduction of a *cyclic prefix* as a *guard interval* (GI), whose length should exceed the maximum excess delay of the multipath propagation channel [9]. Due to the cyclic prefix, the transmitted signal becomes "periodic", and the effect of the time-dispersive multipath channel becomes equivalent to a cyclic convolution, discarding the guard interval at the receiver. Due to the properties of the cyclic convolution, the effect of the multipath channel is limited to a point-wise multiplication of the transmitted data constellations by the channel transfer function, the Fourier transform of the channel impulse response, i.e., the sub-carriers remain orthogonal (see [4]–[7]). This conclusion will also follow from the derivation of the system model in Section 4.2.3. The only drawback of this principle is a slight loss of effective transmit power, as the redundant GI must be transmitted. Usually, the GI is selected to have a length of one tenth to a quarter of the symbol period, leading to an SNR loss of 0.5–1 dB. (See also Figure 4-2).

  The equalization (*symbol de-mapping*) required for detecting the data constella-

tions is an element-wise multiplication of the DFT-output by the inverse of the estimated channel transfer function (*channel estimation*). For phase modulation schemes, multiplication by the complex conjugate of the channel estimate can do the equalization. Differential detection can be applied as well, where the symbol constellations of adjacent sub-carriers or subsequent OFDM symbols are compared to recover the data.

- *Forward error correction* (FEC) coding and (frequency-domain) *interleaving* are the third crucial idea applied. The frequency-selective radio channel may severely attenuate the data symbols transmitted on one or several sub-carriers, leading to bit-errors. Spreading the coded bits over the band-with of the transmitted system, an efficient coding scheme can correct for the erroneous bits and thereby exploit the wide-band channel's frequency-diversity. OFDM systems utilizing error correction coding are often referred as coded OFDM (COFDM) systems. In Chapter 8, the performance of coded OFDM systems is evaluated. The bit-error-rate (BER) of the uncoded system is analyzed in Section 4.3.

The complex equivalent base-band signals generated by digital signal processing are in-phase/quadrature *(I/Q)-modulated* and *up-converted* to be transmitted via an RF-carrier. The reverse steps are performed by the receiver.

Synchronization is a key issue in the design of a robust OFDM receiver. *Time*- and *frequency-synchronization* are paramount to respectively identify the start of the OFDM symbol and to align the modulators' and the demodulators' local oscillator frequencies. If any of these synchronization tasks is not performed with sufficient accuracy, then the orthogonality of the sub-carriers is (partly) lost. That is, inter-symbol-interference (ISI) and inter-carrier-interference (ICI) are introduced. The effect of small synchronization errors is analyzed in Section 4.2.4. Synchronization algorithms are discussed in Chapter 6.

4.2.2 Design of the OFDM Signal

The proposal of a realistic OFDM-based communications system was one of the goals of this research project. Therefore, we elaborate here on some hardware related design considerations, which are often neglected in theoretical studies. Elements of the transmission chain that have impact on the design of the transmitted OFDM signal are:

- The time-dispersive nature of the mobile channel, which the transmission scheme must be able to cope with.
- The bandwidth limitation of the channel. The signal should occupy as little bandwidth as possible and introduce a minimum amount of interference to systems on adjacent channels.
- The transfer function of the transmitter/receiver hardware. This transfer function reduces the useable bandwidth compared to the theoretical one given by the sam-

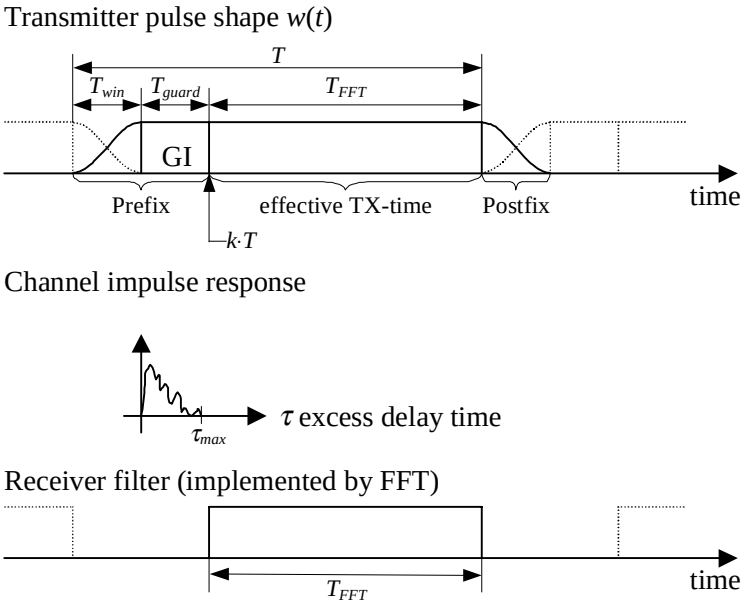

Figure 4-2: Cyclic extension and windowing of the OFDM symbol.

pling theorem. I.e., some oversampling is required.

- Phase-jitter and frequency offsets of the up- and down-converters, and Doppler spreading of the channel.

4.2.2.1 Guard Interval

As mentioned above, a guard interval (GI) is introduced to preserve the orthogonality of the sub-carriers and the independence of subsequent OFDM symbols, when the OFDM signal is transmitted over a multipath radio channel. The guard interval, a cyclic prefix, is a copy of the last part of the OFDM symbol, which is transmitted before the so-called "effective" part of the symbol (*cf.* Figure 4-2). Its duration T_{guard} is simply selected larger than the maximum excess delay of the (worst-case) radio channel. Therefore, the effective part of the received signal can be seen as the cyclic convolution of the transmitted OFDM symbol by the channel impulse response.

4.2.2.2 Windowing

A rectangular pulse has a very large bandwidth due to the side-lobes of its Fourier transform being a sinc-function. Windowing is a well-known technique to reduce the level of these side-lobes and thereby reduce the signal power transmitted out of band. In an OFDM system, the applied window must not influence the signal during its effective period. Therefore, cyclically extended parts of the symbol are pulse-shaped as depicted in Figure 4-2 [3].

Note that this additional cyclic prefix extends the GI to some extent. I.e., the delay-spread robustness is slightly enhanced. On the other hand, the efficiency is further reduced, as the window part is also discarded by the receiver. The orthogonality of the

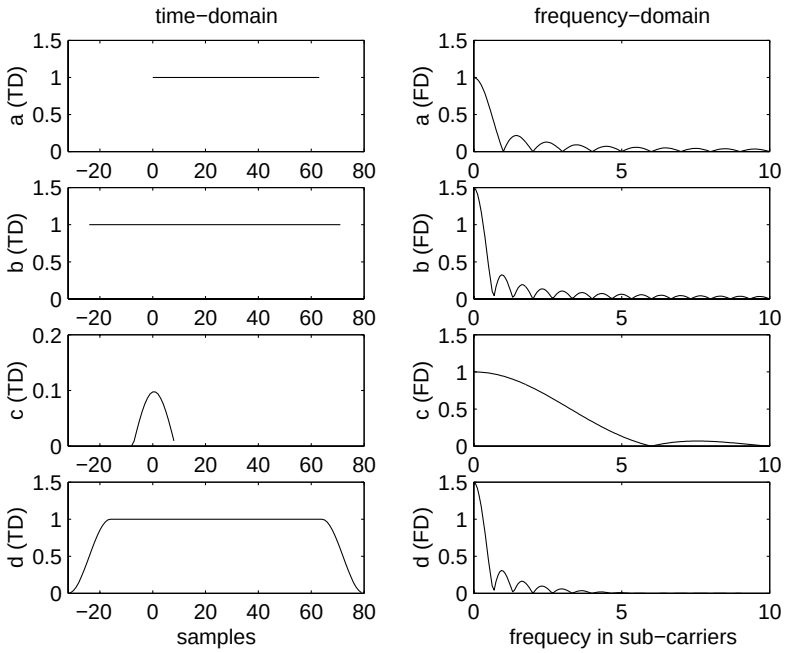

(a) – (d)

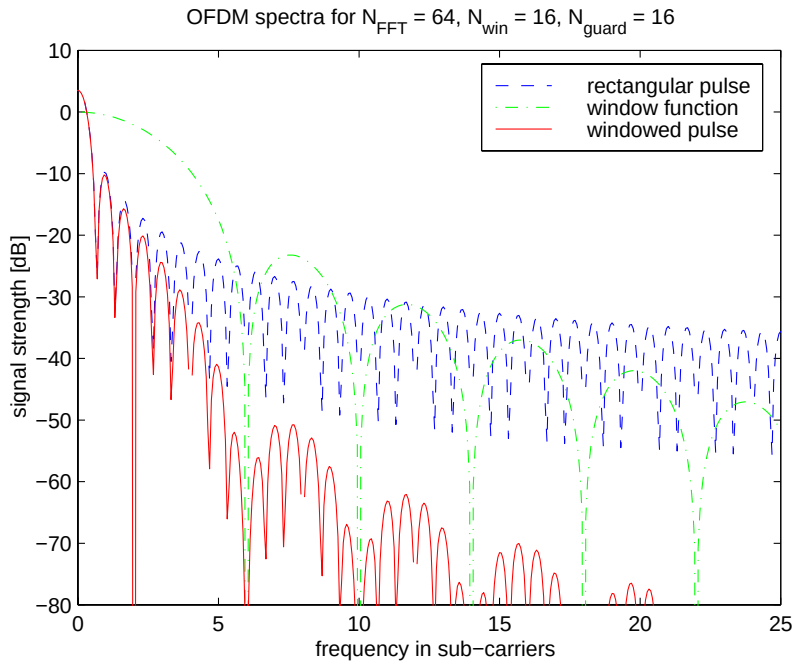

(e)

Figure 4-3: (a): Shape and spectrum of the OFDM receive filter (realized by FFT); (b): rectangular pulse of duration *T* and its spectrum; (c): sine-half-wave used for pulse-shaping and its spectrum; (d): transmitter pulse prototype *w*(*t*) and its spectrum. (e): Spectra of (b)–(d) in logarithmic scale.

sub-carriers of the OFDM signal is restored by the rectangular receiver filter implemented by the DFT (Figure 4-2), requiring the correct estimation of the DFT start time $k \cdot T$, where T is the OFDM symbol period.

The symbol periods in Figure 4-2 are given as times. Since the implementation is usually done on digital hardware, those periods are also often defined in terms of samples. N, N_{guard}, and N_{win} then define the number of samples in the effective part, guard-, and windowing-interval, respectively. The effective part is also referred to as the "FFT-part", because this part of the OFDM symbol is applied to the FFT to recover the data at the receiver.

Spectrum of the transmitter pulse shape

Windowing of the transmitter pulse using a raised-cosine function can be seen as a convolution of the extended rectangular pulse of duration T with a sine-half-wave, as shown in Figure 4-3. In the frequency-domain, this convolution means a multiplication of the sinc-spectrum of the rectangular pulse with the spectrum of the sine-half-wave. It is seen that this multiplication reduces the side-lobes of the transmitter pulse shape.

In Figure 4-3 (a), the zeros of the spectrum occur at positions $i \cdot F = i/T_{FFT}$, $i = \{\pm 1, \pm 2, \ldots\}$, i.e., at those positions, where the adjacent sub-carriers are located. The extension of the rectangular pulse to length $T = T_{FFT} + T_{guard} + T_{win}$ reduces the distance between zeros to $1/T$ (Figure 4-3 (b)). The windowing function (Figure 4-3 (c)) has zeros at positions $\pm 1/T_{win} \cdot \{3/2, 5/2, 7/2, \ldots\}$.

4.2.2.3 System Transfer Function (ADCs, DACs, IF-Filters, RF Front-end, etc.)

Because of the low-pass filters required for the analog-to-digital and digital-to-analog conversion (ADC and DAC) of the transmitted and received (baseband) signals, not all N sub-carriers can be used, if an N-point IFFT is applied for modulation. The sub-carriers close to the Nyquist frequency $f_s/2$ will be attenuated by these filters and thus cannot be used for data transmission (see Figure 4-4). ($f_s = 1/T_s$ is the sampling frequency.) Also the DC-sub-carrier might be heavily distorted by DC offsets of the ADCs and DACs, by carrier feed-through, etc., and should thus be avoided for data.

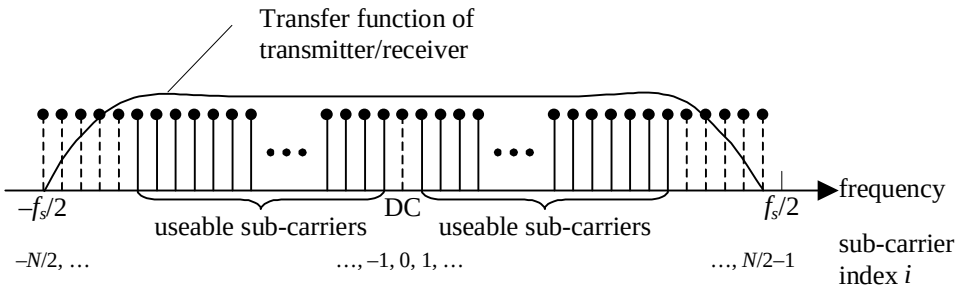

Figure 4-4: Transfer function of the transmitter/receiver hardware and its impact on the design of an OFDM system.

4.2.3 OFDM System Model

The above-introduced features of the OFDM signal are defined mathematically in this section. This will lead to the conclusion that, using the OFDM principle, data symbols

can be transmitted over multipath radio channels without influencing each other.

4.2.3.1 Signal Model and Definitions

Mathematically, the OFDM signal is expressed as a sum of the prototype pulses shifted in the time- and frequency directions and multiplied by the data symbols. In continuous-time notation, the k-th OFDM symbol is written

$$s_{RF,k}(t-kT) = \begin{cases} \mathrm{Re}\left\{ w(t-kT) \sum_{i=-N/2}^{N/2-1} x_{i,k} e^{j2\pi\left(f_c + \frac{i}{T_{FFT}}\right)(t-kT)} \right\} & \\ & kT - T_{win} - T_{guard} \le t \le kT + T_{FFT} + T_{win} \\ 0 & \textit{otherwise} \end{cases} . \quad (4\text{-}1)$$

Most of the mathematical symbols have been defined in the previous figures already. A complete list of symbols is given below:

T	Symbol length; time between two consecutive OFDM symbols
T_{FFT}	FFT-time; effective part of the OFDM symbol
T_{guard}	Guard-interval; duration of the cyclic prefix
T_{win}	Window-interval; duration of windowed prefix/postfix for spectral shaping
f_c	Center frequency of the occupied frequency spectrum
$F = 1/T_{FFT}$	frequency spacing between adjacent sub-carriers
N	FFT-length; number of FFT points
k	index on transmitted symbol
i	index on sub-carrier; $i \in \{-N/2, -N/2+1, \ldots, -1, 0, 1, \ldots, N/2-1\}$
$x_{i,k}$	signal constellation point; complex {data, pilot, null} symbol modulated on the i-th subcarrier of the k-th OFDM symbol

$w(t)$ denotes the transmitter pulse shape defined as

$$w(t) = \begin{cases} \frac{1}{2}\left[1 - \cos\pi(t + T_{win} + T_{guard})/T_{win}\right] & -T_{win} - T_{guard} \le t < -T_{guard} \\ 1 & -T_{guard} \le t \le T_{FFT} \\ \frac{1}{2}\left[1 + \cos\pi(t - T_{FFT})/T_{win}\right] & T_{FFT} < t \le T_{FFT} + T_{win} \end{cases} \quad (4\text{-}2)$$

Finally, a continuous sequence of transmitted OFDM symbols is expressed as

$$s_{RF}(t) = \sum_{k=-\infty}^{\infty} s_{RF,k}(t-kT) \quad (4\text{-}3)$$

The simulated spectrum of such an OFDM signal is depicted in Figure 4-5 for different

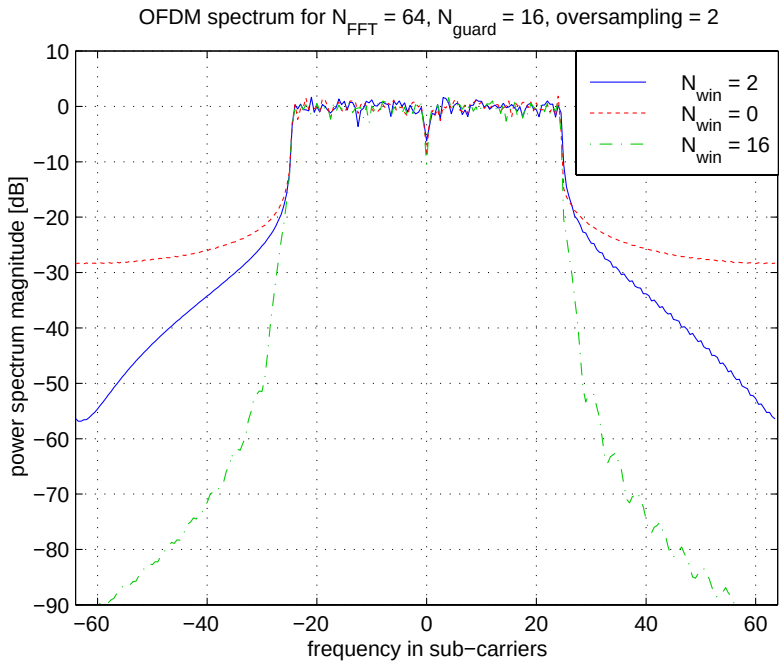

Figure 4-5: Spectrum of an OFDM signal with 64 sub-carriers and different window lengths. Two-fold oversampling has been applied in the time-domain; 48 sub-carriers are used for data.

window lengths.

4.2.3.2 Lowpass Equivalent Transmitted Signal

From eqs. (4-1)–(4-3), the complex equivalent lowpass signal transmitted can be directly given. The complex envelope of the OFDM signal is written

$$s(t) = \sum_{k=-\infty}^{\infty} s_k(t - kT), \tag{4-4}$$

with

$$s_k(t-kT) = \begin{cases} w(t-kT) \sum_{i=-N/2}^{N/2-1} x_{i,k} e^{j2\pi\left(\frac{i}{T_{FFT}}\right)(t-kT)} & kT - T_{win} - T_{guard} \le t \le kT + T_{FFT} + T_{win} \\ 0 & otherwise \end{cases} \tag{4-5}$$

Note the similarities of this expression to the equation of a Fourier series

$$v(t) = \sum_{n=-\infty}^{\infty} c(nf_0) e^{j2\pi n f_0 t}, \tag{4-6}$$

where the complex-valued Fourier coefficients $c(nf_0)$ represent the complex-valued signal constellation points $x_{i,k}$, and the frequencies nf_0 correspond to the sub-carrier

frequencies i/T_{FFT}.

In a digital system, this modulated waveform can be generated by an inverse discrete Fourier transform (IDFT) or by its computationally efficient implementation, the IFFT. The data constellations $x_{i,k}$ are the input to this IFFT; the time-domain OFDM symbol is its output.

4.2.3.3 Time-Dispersive Channel

The influence of the time-variant, multipath fading radio channel is expressed by its (lowpass equivalent) impulse response $h(\tau,t)$ plus AWGN $n(t)$:

$$r(t) = h(\tau,t) * s(t) + n(t) = \int_0^{\tau_{max}} h(\tau,t)s(t-\tau)d\tau + n(t) \tag{4-7}$$

The range of integration in this convolutional integral (* denotes convolution) has been limited to [0, τ_{max}], because the channel impulse response is zero elsewhere. Excess delay $\tau = 0$ of the channel is defined as the delay time at which the first wave arrives at the receiver. Thus, transmit and receive time instants are mathematically defined equal (compare Figure 4-2). τ_{max} is the maximum excess delay of the channel.

Two assumptions are made to simplify the derivation of the received signal. The channel is considered quasi-static during the transmission of the k-th OFDM symbol, thus $h(\tau,t)$ simplifies to $h_k(\tau)$. Furthermore, we define the maximum excess delay $\tau_{max} < T_{guard}$. Therefore, there is no interference of one OFDM symbol on the effective period of the consecutive one (*cf.* Figure 4-2). I.e., inter-symbol-interference (ISI) is suppressed in case of sufficiently accurate time synchronization.

4.2.3.4 OFDM Demodulation

The demodulation of the OFDM signal should be performed by a bank of filters, which are "matched" to the effective part [kT, $kT + T_{FFT}$] of the OFDM symbol (see Figure 4-2). The reverse operation to eq. (4-6), i.e., the extraction of the Fourier coefficients $c(nf_0)$ (= $x_{i,k}$) from the time-domain signal $v(t)$ (= $r(t)$), exactly formulates such a bank of matched filters. It is written

$$c(nf_0) = \frac{1}{T_0}\int_{T_0} v(t)e^{-j2\pi nf_0 t}dt\,, \tag{4-8}$$

where T_0 is the integration period being equivalent to T_{FFT}. In a digital implementation, a DFT or (preferably) a FFT is used to realize these filters.

Assuming knowledge of the exact time-instants kT at which the OFDM symbols start, we try to extract the transmitted signal constellations $x_{i,k}$ from the received signal $r(t)$. The received signal constellations are denoted $y_{i,k}$.

$$y_{i,k} = \frac{1}{T_{FFT}} \int_{t=kT}^{kT+T_{FFT}} r(t) e^{-j2\pi i (t-kT)/T_{FFT}} dt = \frac{1}{T_{FFT}} \int_{t=kT}^{kT+T_{FFT}} \left[\int_{\tau=0}^{\tau_{max}} h_k(\tau) s(t-\tau) d\tau + n(t) \right] e^{-j2\pi i (t-kT)/T_{FFT}} dt \tag{4-9}$$

Because of the integration ranges in eq. (4-9) and $\tau_{max} < T_{guard}$, there is no influence of the adjacent OFDM symbols transmitted, and $s(t)$ can be replaced by $s_k(t)$, eq. (4-5).

$$y_{i,k} = \frac{1}{T_{FFT}} \int_{t=kT}^{kT+T_{FFT}} \left[\int_{\tau=0}^{\tau_{max}} h_k(\tau) \sum_{i'=-N/2}^{N/2-1} x_{i',k} e^{j2\pi \left(\frac{i'}{T_{FFT}} \right) (t-kT-\tau)} d\tau \right] e^{-j2\pi i (t-kT)/T_{FFT}} dt + \frac{1}{T_{FFT}} \int_{t=kT}^{kT+T_{FFT}} n(t) e^{-j2\pi i (t-kT)/T_{FFT}} dt \tag{4-10}$$

Note that $w(t - kT) = 1$ in the range of integration. The window is thus omitted in this equation. The second integral in eq. (4-10) leads to independent additive noise samples $n_{i,k}$ since the complex exponential terms represent orthogonal functions. Substituting $u = t - kT$, for the ease of notation, and changing the order of integration and summation yields

$$y_{i,k} = \sum_{i'=-N/2}^{N/2-1} x_{i',k} \frac{1}{T_{FFT}} \int_{u=0}^{T_{FFT}} \left[\int_{\tau=0}^{\tau_{max}} h_k(\tau) e^{j2\pi i'(u-\tau)/T_{FFT}} d\tau \right] e^{-j2\pi i u/T_{FFT}} du + n_{i,k} = \sum_{i'=-N/2}^{N/2-1} x_{i',k} \frac{1}{T_{FFT}} \int_{u=0}^{T_{FFT}} \left[\int_{\tau=0}^{\tau_{max}} h_k(\tau) e^{-j2\pi i'\tau/T_{FFT}} d\tau \right] e^{-j2\pi (i-i')u/T_{FFT}} du + n_{i,k} \tag{4-11}$$

The inner integral of the second expression represents the Fourier transform of $h_k(\tau)$ at the frequency instants $i'/T_{FFT} = i'F$, which is the sampled channel transfer function at time kT. It is expressed by the channel coefficients

$$h_{i',k} = FT\{h_k(\tau)\} = \int_{\tau=0}^{\tau_{max}} h_k(\tau) e^{-j2\pi i'\tau/T_{FFT}} d\tau = H(i'F, kT). \tag{4-12}$$

Using this notation, the output of the receiver filter bank simplifies to

$$y_{i,k} = \sum_{i'=-N/2}^{N/2-1} x_{i',k} h_{i',k} \frac{1}{T_{FFT}} \int_{u=0}^{T_{FFT}} e^{-j2\pi (i-i')u/T_{FFT}} du + n_{i,k} \tag{4-13}$$

The integral in this equation has the value 1, only if $i = i'$. For $i \neq i'$, i and i' being integer values, the integral is zero. Thus we finally obtain

$$y_{i,k} = x_{i,k} h_{i,k} + n_{i,k}. \tag{4-14}$$

From this form it is seen that a perfectly synchronized OFDM system can be viewed as a set of parallel Gaussian channels as depicted in Figure 4-6 [4]–[6]. The multipath

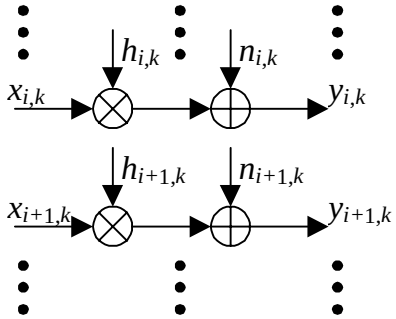

Figure 4-6: Idealized OFDM system model. The sub-channels of the OFDM system can be considered as parallel Gaussian channels under the assumptions of perfect time- and carrier synchronization and perfect suppression of multipath by the guard interval.

channel introduces an attenuation/amplification and phase rotation according to the (complex-valued) channel coefficients $\{h_{i,k}\}$.

Channel estimation is required in order to retrieve the data contained in these signal constellations, because the receiver must have a phase (and amplitude) reference to correctly detect the transmitted symbol. Differential detection can be used alternatively, in which case the decision is made by comparing the phases (and amplitudes) of symbols transmitted over adjacent sub-carriers or subsequent OFDM symbols.

Due to the attenuation/amplification, each sub-carrier typically has an individual signal-to-noise ratio (SNR). The SNR per sub-carrier (after the DFT) is defined as

$$(E_c / N_0)_{i,k} = E\{|x_{i,k}|^2\}\left|h_{i,k}\right|^2 \big/ \sigma_N^2 , \tag{4-15}$$

where $\sigma_N^2 = E\{|n_{i,k}|^2\}$ is the noise variance. With the normalized received power being written $P_0 = E\{|h_{i,k}|^2\}$, the average SNR becomes $\overline{E_c / N_0} = E\{|x_{i,k}|^2\} P_0 / \sigma_N^2$. Usually, the signal energy is normalized to unity, i.e., $E\{|x_{i,k}|^2\} = 1$.

4.2.4 Synchronization Errors

As an introduction to the work on synchronization algorithms, the relevant effects of synchronization errors are reviewed in this section. Original work on this topic is found in numerous publications (see e.g. [10], [11]). A comprehensive overview is given in [7].

4.2.4.1 FFT Time Synchronization Error

The impact of an FFT-timing offset at the receiver can be analyzed mathematically by shifting the integration interval of the matched filter bank, eq. (4-9). For a timing error of δt, the ideal interval $t \in [kT, kT + T_{FFT}]$ becomes $t \in [kT + \delta t, kT + T_{FFT} + \delta t]$ and (4-9) is written

$$y_{i,k} = \frac{1}{T_{FFT}} \int_{t=kT+\delta t}^{kT+T_{FFT}+\delta t} r(t) e^{-j2\pi i (t-kT-\delta t)/T_{FFT}} dt \tag{4-16}$$

δt is assumed to be sufficiently small (typically $\delta t < T_{guard}$) that no ISI arises due to the timing error. In other words, the error is small enough for the channel impulse response to remain within the guard interval. Therefore, the receiver window still does not overlap with the preceding or consecutive OFDM symbol, i.e., no energy is collected from these adjacent OFDM symbols, and the demodulated signal can be expressed from the transmitted symbol $s_k(t)$ again (compare eq. (4-10)). Following the same steps as in Section 4.2.3 (eqs. (4-9)–(4-14)), we obtain for the second part of eq. (4-11) (with $u = t - kT - \delta t$),

$$y_{i,k} = \sum_{i'=-N/2}^{N/2-1} x_{i',k} \frac{1}{T_{FFT}} \int_{u=0}^{T_{FFT}} \left[\int_{\tau=0}^{\tau_{max}} h(\tau) e^{-j2\pi i'\tau/T_{FFT}} d\tau \right] e^{-j2\pi[(i-i')u + i'\delta t]/T_{FFT}} du + n_{i,k} \tag{4-17}$$

Moving the term $e^{-j2\pi i'\delta t/T_{FFT}}$ out of the integral yields the expression for the demodulated signal constellations in case of a timing error,

$$y_{i,k} = x_{i,k} h_{i,k} e^{-j2\pi i \delta t/T_{FFT}} + n_{i,k} = x_{i,k} h_{i,k} e^{-j2\pi i \delta t'/N} + n_{i,k}\,, \tag{4-18}$$

where $\delta t'$ is the timing offset in samples. It is evident that a timing offset gives rise to a progressive phase rotation of the signal constellations. The phase rotation is zero at the center frequency and it linearly increases towards the edges of the frequency band. It is easily verified from eq. (4-18) that a timing-offset of one sample introduces a phase shift of $\pm\pi$ to the outermost sub-carriers (having $i \cong \pm N/2$), regardless of the FFT-length. In Figure 4-7, this effect is visualized for a 64-carrier OFDM system with zero carriers at f_c and at the edges of the frequency band.

If coherent detection is utilized, the induced progressive phase rotation is detected implicitly by the channel estimation algorithm. The subsequent equalization (sub-carrier-wise multiplication of the received symbols by the inverse of the estimated channel coefficients) will thus automatically correct for small timing-offsets. No performance degradation is thereby caused. However, if the timing offset is too large, ISI and ICI are introduced because energy is also collected from one of the adjacent OFDM symbols, leading to a partial loss of orthogonality [7].

Differential detection is also robust to small timing-offsets. If the differential detection is applied in the frequency-direction, the progressive phase rotation may reduce the distance between the compared constellation points, however, which can lead to a performance degradation. Such performance results are given in Section 4.3.3.

A (small) *sampling* frequency offset leads to a (slowly) increasing timing offset, and therefore to a progressive phase rotation at an increasing slope. Larger errors yield ICI, because the SC-spacing at the receiver can no longer be assumed equal to the SC-spacing at the transmitter. (The SC-spacing is defined as $F = 1/(NT_s)$, where T_s is the

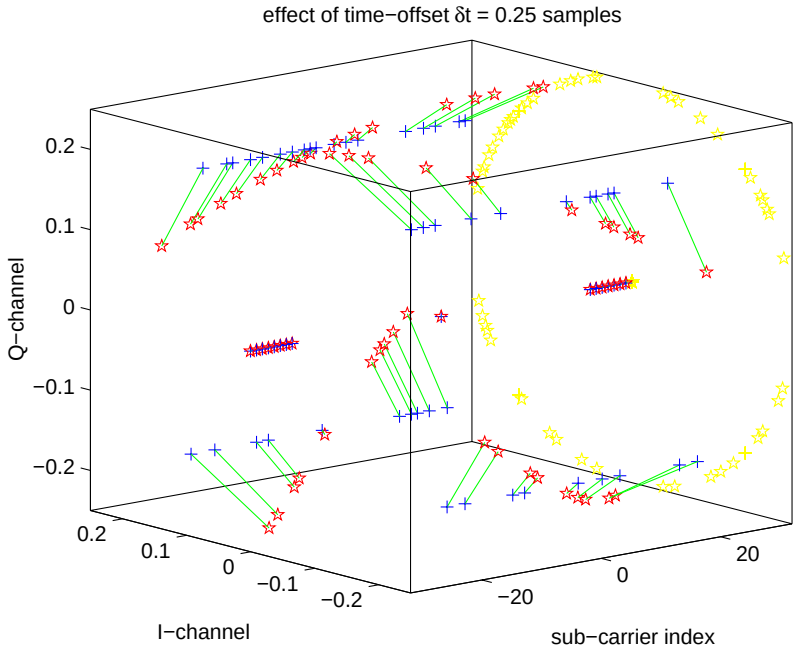

Figure 4-7: Visualization of the influence of an FFT timing offset on the demodulated signal constellations. A linearly increasing phase rotation is observed with increased frequency distance to the center frequency. '+' indicate QPSK constellations without the influence of a timing-offset; '☆' depict the rotated data symbols.

sampling period.)

4.2.4.2 Carrier Synchronization Error

Frequency offsets are typically introduced by a (small) frequency mismatch in the local oscillators of the transmitter and the receiver. Doppler shifts can be neglected in indoor environments.

The impact of a frequency error can be seen as an error in the frequency instants, where the received signal is sampled during demodulation by the FFT. Figure 4-8 depicts this two-fold effect. The amplitude of the desired sub-carrier is reduced ('+') and inter-carrier-interference ICI arises from the adjacent sub-carriers ('○').

Mathematically, a carrier offset can be accounted for by a frequency shift δf and a phase offset θ in the lowpass equivalent received signal

$$r'(t) = r(t)e^{j(2\pi\delta f t+\theta)}. \tag{4-19}$$

With eq. (4-9) we obtain

$$y_{i,k} = \frac{1}{T_{FFT}} \int_{t=kT}^{kT+T_{FFT}} r(t)e^{j(2\pi\delta f t+\theta)}e^{-j2\pi i(t-kT)/T_{FFT}}dt = e^{j2\pi\theta}\frac{1}{T_{FFT}}\int_{t=kT}^{kT+T_{FFT}}\left[\int_{\tau=0}^{\tau_{max}} h(\tau)s(t-\tau)d\tau + n(t)\right]e^{j2\pi\delta f t}e^{-j2\pi i(t-kT)/T_{FFT}}dt \tag{4-20}$$

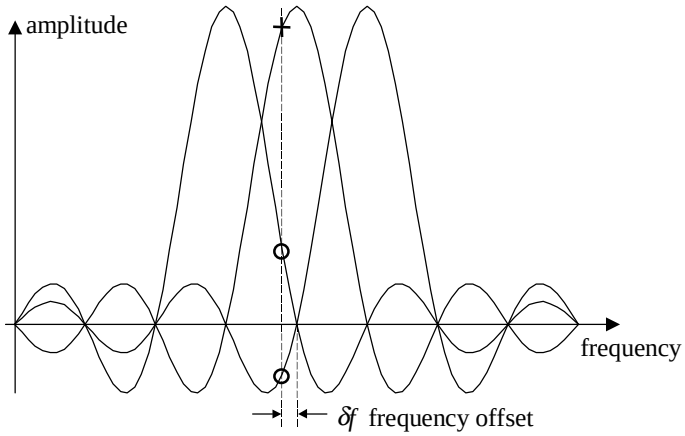

Figure 4-8: Inter-carrier-interference (ICI) arises in case of a carrier synchronization error. The figure illustrates the spectra of three individual sub-carriers. These spectra are superimposed in the OFDM signal spectrum.

Repeating the derivation leading to eq. (4-13), the received constellation points become

$$y_{i,k} = e^{j(\theta+2\pi\delta fkT)} \sum_{i'=-N/2}^{N/2-1} x_{i',k} h_{i',k} \frac{1}{T_{FFT}} \int_{u=0}^{T_{FFT}} e^{-j2\pi(\frac{i-i'}{T_{FFT}}-\delta f)u} du + n_{i,k} \,. \tag{4-21}$$

Due to the frequency error, the integral is not equal zero for $i \neq i'$, neither it is one for $i = i'$, as in the idealized case above. I.e., the orthogonality between sub-carriers has been partly lost. The evaluation of this expression yields two terms. The first term (for $i = i'$) accounts for equal phase rotation and attenuation of all sub-carriers, the second one (for $i \neq i'$) describes the ICI.

$$\begin{aligned} y_{i,k} = {} & e^{j(\theta+2\pi\delta fkT)} x_{i,k} h_{i,k} \frac{1}{T_{FFT}} \int_{u=0}^{T_{FFT}} e^{j2\pi\delta fu} du + \\ & e^{j(\theta+2\pi\delta fkT)} \sum_{\substack{i'=-N/2 \\ i'\neq i}}^{N/2-1} x_{i',k} h_{i',k} \frac{1}{T_{FFT}} \int_{u=0}^{T_{FFT}} e^{-j2\pi(\frac{i-i'}{T_{FFT}}-\delta f)u} du + n_{i,k} \end{aligned} \tag{4-22}$$

These expressions are valid for a frequency-offset $\delta f < 0.5$ SC. For larger offsets, the transmitted data symbols $x_{i,k}$ would get shifted by one or more positions in the frequency-direction. I.e., the data symbol of the i-th transmitted SC would appear at the $(i + \delta f_i)$-th SC at the receiver, where $\delta f_i = \text{round}(\delta f/F)$ is the integer part of the frequency-error in sub-carriers.

The ICI term can be seen as an additional noise term and can thus be represented as a degradation of SNR. The amount of degradation has been evaluated by Pollet *et al.* [10] for AWGN channels and by Moose [11] for dispersive fading channels (see also [7]). Frequency-offsets up to 2 % of the sub-carrier spacing F are negligible, according to their results. Even 5–10 % can be tolerated in many situations.

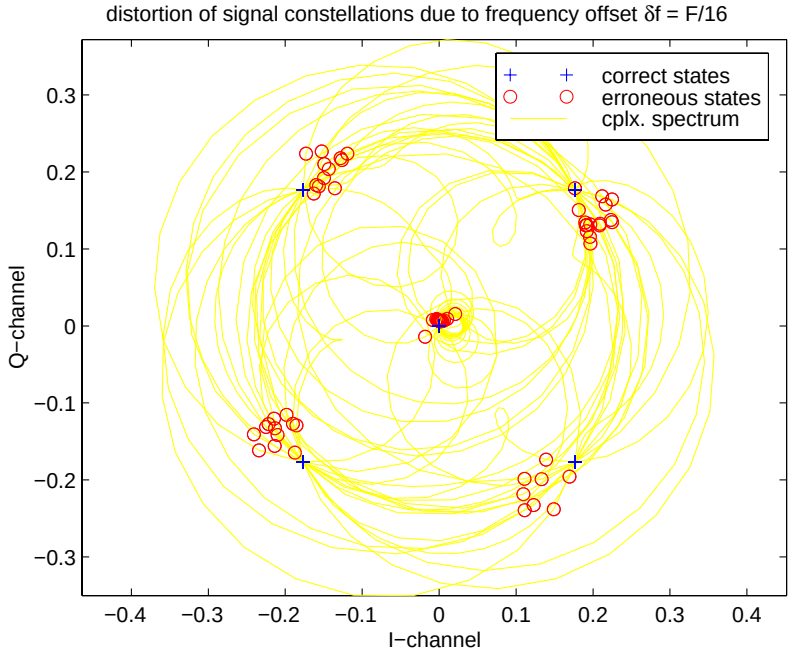

Figure 4-9: Phase rotation due to carrier offset of 1/16 of the sub-carrier spacing. The received signal constellations distorted by ICI are shown.

Evaluation of the phase rotation and attenuation due to a frequency error yields

$$y_{i,k} = x_{i,k} h_{i,k} \operatorname{sinc}(\delta f \, T_{FFT}) \exp\{j[\theta + 2\pi\delta f \, (kT + T_{FFT}/2)]\} + n'_{i,k}\,, \tag{4-23}$$

using

$$\frac{1}{T_{FFT}} \int_{t=0}^{T_{FFT}} e^{j2\pi\delta f t} dt = \frac{1}{j2\pi\delta f T_{FFT}} \left[e^{j2\pi\delta f T_{FFT}} - 1\right] = e^{j\pi\delta f T_{FFT}} \frac{\sin \pi\delta f T_{FFT}}{\pi\delta f T_{FFT}} = e^{j\pi\delta f T_{FFT}} \operatorname{sinc} \delta f T_{FFT}\,. \tag{4-24}$$

The noise term $n'_{i,k}$ includes the additional noise due to ICI.

Figure 4-9 depicts the rotation and distortion of the received signal constellation points for a carrier offset of $\delta f = F/16$, $\theta = 0$, and for QPSK modulation ('○'). The scattering of the resulting complex valued signal constellations is caused by ICI. The figure also shows the projection of the continuous Fourier spectrum of one OFDM symbol on the complex plane, i.e., the spectrum in-between the sub-carrier frequencies. This line results from the superposition of the continuous sinc-spectra of individual sub-carriers of one OFDM symbol. If a frequency-offset is present, the DFT samples this spectrum at the wrong frequency-instants – leading to ICI –, which is indicated in the figure by '○'. Without frequency-offset, the QPSK constellations are recovered perfectly, as seen from the points marked by '+'.

4.2.4.3 Common Carrier and Timing Offset

Evaluating the above expressions for simultaneous timing (δt), frequency (δf, $\delta f_i = \text{round}(\delta f/F)$) and phase ($\theta$) offsets, the system model for the generalized case is

obtained. It is written as

$$y_{i+\delta i,k} = x_{i,k} h_{i,k} \operatorname{sinc}\left[(\delta f - \delta f_i F) T_{FFT}\right] e^{j\Psi_{i,k}} + n'_{i,k}, \tag{4-25}$$

where the phase distortion due to the synchronization errors is expressed by

$$\Psi_{i,k} = \theta + 2\pi\delta f\left(kT + \frac{T_{FFT}}{2} + \delta t\right) + 2\pi\delta t \frac{i}{T_{FFT}}. \tag{4-26}$$

Note again that the noise variable $n'_{i,k}$ in (4-25) includes the noise caused by ICI and/or ISI.

Often, the timing offset is expressed in samples, i.e., $\delta t' = \delta t/T_s$, and the frequency-offset is normalized to the sub-carrier spacing $\delta f' = \delta f / F$. Using these symbols, the phase distortions are expressed by

$$\Psi_{i,k} = \theta + 2\pi\delta f'\left(\frac{1}{2} + k\frac{N + N_{guard} + N_{win}}{N} + \frac{\delta t'}{N}\right) + 2\pi\delta t' \frac{i}{N}. \tag{4-27}$$

4.4 Conclusions and Recommendations

The derivation of the OFDM system model has confirmed that data symbols can be transmitted independently over multipath fading radio channels. It has to be assumed, however, that the channel's maximum excess delay is shorter than the guard interval, and that the system has been synchronized sufficiently. Small synchronization errors lead to systematic phase rotations of the data constellation points – a property which can be exploited for estimating synchronization offsets. If the timing- or frequency-synchronization error becomes too large, the orthogonality of the sub-carriers is partly lost and the signal-to-noise ratio of the system is degraded. That is, inter-carrier-interference (ICI) and inter-symbol-interference arise. ICI can also result from very fast channel variations (Doppler spreads) or from carrier phase jitters.

The system models presented can be utilized in analytical studies of various aspects of the OFDM technique, as, for instance, in the performance evaluation. The basic model introduced assumes perfect synchronization, while an extended model considers the phase rotations due to small synchronization-offsets.

4.5 References

[1] J. G. Proakis, *Digital Communications*, 3rd edition. New York: McGraw Hill, 1995.

[2] R. Prasad, *Universal Personal Communications*. Boston: Artech house, 1998, ch. 10.

[3] R. van Nee and R. Prasad, *OFDM for Wireless Multimedia Communications*. Boston: Artech House, 2000.

[4] O. Edfors, M. Sandell, J. J. van de Beek, D. Landström, F. Sjöberg, "An Introduction to Orthogonal Frequency-Division Multiplexing," *Research Report TULEA 1996:16*, Division of Signal Processing, Luleå University of Technology, http://www.sm.luth.se/ csee/sp/publications.html.

[5] O. Edfors, *Low-complexity algorithms in digital receivers*, Ph.D. Thesis, Luleå University of Technology, Sept. 1996.

[6] M. Sandell, *Design and Analysis of Estimators for Multicarrier Modulation and Ultrasonic Imaging*, Ph.D. Thesis, Luleå University of Technology, Sept. 1996.

[7] M. Speth, S. A. Fechtel, G. Fock, and H. Meyr, "Optimum Receiver Design for Wireless Broad-Band Systems Using OFDM–Part I," *IEEE Trans. Commun.*, vol. 47, no. 11, pp. 1668–1677, Nov. 1999.

[8] S. B. Weinstein and P. M. Ebert, "Data Transmission by Frequency-Division Multiplexing Using the Discrete Fourier Transform," *IEEE Trans. Commun. Techn.*, vol. COM-19, no. 5, pp. 628–634, Oct. 1971.

[9] A. Peled and A. Ruiz, "Frequency Domain Data Transmission Using Reduced Computational Complexity Algorithms, " *in Proc. IEEE Int. Conf. Acoust., Speech, Signal Processing*, Denver, CO, 1980, pp. 964–967.

[10] P. Pollet, M. van Bladel, and M. Moenclaey, "BER Sensitivity of OFDM Systems to Carrier Frequency Offset and Wiener Phase Noise," *IEEE Trans. on Commun.*, vol. 43, no. 2/3/4, pp. 191–193, Feb./March/April 1995.

[11] P. H. Moose, "A technique for orthogonal frequency division multiplexing frequency offset correction," *IEEE Trans. Commun.*, vol. 42, no. 10, pp. 2908–2914, Oct. 1994.

[12] P. A. Bello, "Characterization of randomly time-variant linear channels," *IEEE Trans. on Commun. Systems*, vol. CS-11, pp. 360–393, Dec. 1963.

[13] R. Steele, *Mobile Radio Communications.* New York: John Wiley & Sons, 1992.

[14] W. C. Jakes Jr., *Microwave Mobile Communications*. New York: John Wiley & Sons, 1974.